Eng. & Tech. Journal, Vol.30 , No.15, 2012

Method for Shielding the Magnetic Field Generated in a 132/33/11(6.6)kV Baghdad Indoor Distribution Substation

Dr. Suad I. Shahl
Electrical Engineering Department, University of Technology/Baghdad
Email: suad732002 @yahoo.com

Received on: 30/11/2011 & Accepted on: 7/6/2012

ABSTRACT

This research introduces the study carried out on one of Baghdad East 132/33/11(6.6) kV distribution substations to mitigate 50Hz magnetic field of indoor distribution substation under normal operation. Shielding was performed at the power sources such as busbars rather than at the affected areas. Three-dimensional finite element method (FEM) is used to calculate the magnetic field density in the space nearby the busbars so as to analyze the shielding effectiveness of an eddy current shield applied to a 132/33/11(6.6)kV substation. It also deals with the influence of shield distance from busbar, thickness and material of shield on the eddy current losses and shielding efficiency applied to 3D finite element model of a particular busbar configuration.

Keywords: Magnetic fields, Eddy current, Finite Element Method (FEM), shielding, Substation

طريقة للحماية من المجال المغناطيسي المتولد في داخل محطة توزيع ثانوية 132/33/11(6.6)kV في بغداد

الخلاصة

يقدم هذا البحث دراسة نفذت على احدى محطات التوزيع الثانوية 133/33/11(6.6)kV في شرق بغداد للتخفيف من المجال المغناطيسي ذي التردد (50Hz) داخل محطة التوزيع ثانوية تحت ظروف التشغيل الطبيعي. نفذت الحماية عند مصادر الطاقة مثل القضبان العمومية بدلا من المناطق المتأثرة. استخدمت طريقة العنصر المحدود ثلاثية الابعاد في حساب كثافة المجال المغناطيسي في الفضاء القريب من القضبان العمومية لكي نحلل فعالية درع وقاية التيارات الدوامة المسلط على المحطة الثانوية 133/33/11(6.6)kV. حيث يتعامل هذا البحث مع تأثير المسافة بين الدرع الواقي و القضيب العمومي, سمك ومادة معدن الدرع الواقي على خسائر التيار الدوام وكذلك كفاءة الحماية لترتيب معين لقضيب عمومي بأعتماد نموذج ثلاثي الابعاد للعنصر المحدود.

NTRODUCTION

Today electromagnetic environment problem caused by all electrical structures of the electric substation e.g., switching equipment, busbars, feeding lines, VAR compensation, and power cables is paid more attention[1,2]. Therefore, it is necessary to analyze the distribution of magnetic field near/inside high voltage substation especially at the level of human body above the ground in the working area. How to reduce the magnetic field intensity produced has been a hot issue in the field of environmental protection. The problem is how an efficient technique can be developed for shielding of this undesirable influence of electromagnetic field. During the years, to the recent days several papers have been published investigating different types of shielding and determining their efficiency in magnetic field reduction [3-6].

An accurate simulation of shielding problems implies numerical techniques capable of modeling the shape of the extremely low frequency sources and of the conducting plates at the same time. Several specific methods have been proposed in the literature to cope with these requirements. Most of them are based on two-dimensional (2D) electromagnetic field analysis, which provides useful results for some preliminary evaluations at the design stage only [7]. In fact the 2D assumption on geometries strongly limits the applicability of these methods to practical cases. Thus, a three-dimensional (3D) approach is needed to perform a reliable analysis of the shield effectiveness.

This work presents a way using the 3D-FEM to calculate the magnetic field in a 132/33/11(6.6)kV indoor distribution substation in east Baghdad and to investigate the effect of a metal plate on the magnetic field generated by the busbars. ANSYS Commercial Software is employed in this work to assess the magnetic field distribution near/under high voltage busbar in indoor substation and to estimate the effect of eddy currents in shielding materials.

SYSTEM MODELING

To evaluate and simulate the magnetic field produced by high voltage overhead busbars, incoming and outgoing feeders inside 132/33/11(6.6) kV Gas Insulated Switchgear (GIS) substation is chosen; located in the East of Baghdad, Iraq. The specifications of this substation were prepared by the Iraq Ministry of Electricity such as the ratings and numbers of transformers and switchgear circuits [8].

The investigated area under study in this work is simulated as finite element model as shown in Figure1, which shows the arrangement of busbars, vertical connectors, incoming and outgoing feeders inside substation. Table(1) lists parameters of finite element model and material properties of section of each phase from each busbar.

MATHEMATICAL FORMULATION

In general, fields are divided to eddy current field and un-eddy current field in the 3D eddy current field analysis. Time varying electric field and magnetic field are considered in the eddy current field while magnetic field is only considered in the un-eddy current field.

Combinations by vector potential(A) and scalar potential($\emptyset$) are demanded in the eddy current area, while in the un-eddy current area, vector potential or scalar potential is required $\emptyset - A$ method based on vector magnetic potential A is chosen. The method quoting coulomb criterion $\nabla . A = 0$ will source current introduce to un-eddy current area. Therefore, uniquenesses of A and $\emptyset$ get assurance. Equations of eddy current area are given as follows [9, 10]:

$$\nabla \times \frac{1}{\mu} \nabla \times A - \nabla \frac{1}{\mu} \nabla . A \ + \sigma(j\omega A + \nabla \emptyset) = 0 \qquad \ldots (1)$$

$$\nabla . \sigma(-j\omega A - \nabla \emptyset) = 0 \qquad \ldots (2)$$

The governing equations for vectors of magnetic field B and electric field E in a quasistatic system are:

$$B = \nabla \times A, \quad E = -j\omega A - \nabla \emptyset \qquad \ldots (3)$$

Equations of un-eddy current area are given as follows:

$$\nabla \times \frac{1}{\mu} \nabla \times A - \nabla \frac{1}{\mu} \nabla . A \ = J_s \qquad \ldots (4)$$

Where J_s the current density

$$B = \nabla \times A \qquad \ldots (5)$$

where μ and $\boldsymbol{\sigma}$ are the permeability and the conductivity of the material, respectively, and $\boldsymbol{\omega}$ is the angular frequency. The FEM was used for the numerical solution of the vector potential A and scalar potential $\emptyset$.

MODELING OF MAGNETIC SHIELDING

Shielding of magnetic field is extremely complex for extremely low frequency (ELF) broadband (30…300Hz), of minor deformation in materials [11]. The shielding effectiveness *(SE)* is defined as relationship of the field results without shielding and with shielding [12]:

$$SE = 20 log_{10} \frac{B_o}{B_s}$$

where B_o is magnetic flux density without the shield and B_s with the shield.

The problem of shielding extremely low frequency 50 Hz is very complex with thin finite plates for a three-phase system of busbars. As a result of this, to model passive shielding using metal plate numerical methods must be used, since an accurate study of finite, open shields by analytical methods is difficult.

In this study, 3D-FEM is used to model passive shielding and to simulate the field produced by a shielding plate. Shielding was applied to the bus bar with

highly conductive material (aluminum and copper) or with ferromagnetic material (iron). Figure(2) presents the FE model arrangement of the shield and the bus bars. The passive metal plate of width x_S, thickness y_S and length z_S is placed at passive distance d from the phase busbar. In Figure 2 the length of the busbar section is long as compared to the one of the plate $l > z_S$. Different material properties and dimensions of shield considered in the modeling of our system are presented in Table (2).

RESULTS AND DISCUSSION

Numerical Analysis of Magnetic Field Without Shielding

Suppose the balanced three-phase current (2000A, 50Hz) per phase in the model presented in this work. Furthermore, the height of a typical worker (human body) is assumed to be 1.75 m. Therefore in this work the computation for magnetic field is conducted at 1m as average height from the ground. Figure 3 shows the magnetic field (r.m.s) values on the points positioned at 1m above the floor of the indoor substation room on the vertical plane XY.

Figure (4) shows the distribution of height level of magnetic field density on the length along busbars and ingoing/outgoing feeders sections on the horizontal plane XZ in zone under study.

Numerical Analysis of Magnetic Field With Shielding

Different shield configurations have been analyzed by the 3D FEM in order to identify the best shielding solutions, which are depended on cost-mitigation levels of field originated from busbar system.

Figure (5) shows the variation of the magnetic field at the level y=1meter above the floor for three different shielding materials, conductive (copper and aluminum) and ferromagnetic materials.

It is clear that the best shielding material was copper, because its conductivity is the highest. But considering the economic and technical aspects, aluminum was the best choice for shielding material. At the same location, shielding Aluminum clearly shows a better field the variation of the mitigation field according to the distance from center source (busbars) comparison with shielding Ferromagnetic.

Figure (6) shows the variation of the mitigated field levels according to the thickness of the Aluminum plate in the cross section of plane XY for the model under this case study. It is clear that the mitigated field levels decreases with increase the shielding plate thickness (τ).

Figure (7) shows the dependence of the mitigated field on the distance *(d)* between plate and the busbars. The field mitigation increases as the shield comes closer to the busbars.

Analysis of Eddy Currents And Losses on Shielding Plate

Reflection or diffraction of the magnetic field around the shield produces eddy currents on the side of the plate located in front of the system of busbar under study. This effect is more evident as the separation between plate and busbar *(d)* increases, as shown in Figure 8. With current density increased, eddy current loss is shown increasing trend, it can be observed in Figure 9 the 3D eddy current power loss is higher for smaller value of *d*.

Figures (10 and 11) show the effect of the thickness of the Aluminum plate on the eddy current density and eddy current power loss. The results show the eddy current density drops rapidly as the thickness increases, as that the reduction of losses is even more rapid with increasing thickness.

Shielding Effectiveness

Table (3) shows the efficiency of the shielding aluminum plate verses the distance d from the source (busbar model) is calculated at different positions in the cross section of plane XY.

The results prove a smaller shielding effectiveness means a better magnetic field reduction. The shielding effectiveness above 1dB mean that there is actually an enhancement of the magnetic field. The reason for this can be explained by considering the field points not too far from the horizontal centerline; the magnetic field on a horizontal plane above the source busbars is nearly parallel to the plane.

Table (4) shows the efficiency of the shielding aluminum plate verses the thickness τ of shielding plate is calculated at different positions in the cross section of plane XY. It is clear from Table (4) that the shielding effectiveness is higher when the shielding of aluminum (3mm-thick plate).

CONCLUSIONS

The present work is concerned with shielding of 3-D magnetic field inside 132/33/11kV GIS substation in East of Baghdad City/Iraq. The 3D eddy current and power loss due to reflection or diffraction of the magnetic field in a shielding conductive plate were investigated by FEM. Modeling variables included different shielding metal plates and two parameters of the geometric configuration: the plate thickness and the distance from the busbar system.

This work showed that it is possible to achieve cost-effective mitigation of 50Hz magnetic field down to sub-microtesla levels. The field of busbars can be shielded by a thin aluminum plate, symmetrically located and at a small distance.

The technique used in this work can readily be applied to operative substations, comparison with others can only be applied during the design stages. This technique is simple and not very costly to implement in comparison to the shielding of extensive areas.

REFERENCES

[1]. Pretorius, PH, britten AC., "ELF Magnetic Fields in Close Proximity to A Large Static VAR Compensator: A Case Study", IEEE AFRICON 4th, Vol.2, pp.1056-1061, 1996.

[2]. Wong, PS, Rind TM, Harvey SM, Scheer RR, "Power Frequency Electric and Magnetic Fields from a 230kv GAS-Insulated Substation", IEEE Transactions on Power Delivery, Vol.9,issue 3, pp. 1494-1501, 1994.

[3]. Ener Salinas, "Passive and Active Shielding of Power-Frequency Magnetic Fields from Secondary Substation Components", IEEE International Conference on Power System Technology, Vol.2, pp.855-860, (4-7) Dec.2000.

[4]. M. Istenič, P. Kokelj, P. Žunko, B. Cestnik, T. Živic, "Some Aspects of Magnetic Shielding of a Transformer Substation Using Alternative Shielding

Techniques", IEE 16th International Conference and Exhibition on Electricity Distribution Part 1, Vol.2, pp.1-5, (18 21)Jun.2001.

[5]. Ruan Jiangjun, Huang Jinghui, Chen Yunping, Liu Qisheng, "Shielding Effectiveness of Shielding Cabinet in Substation with 3D Eddy Current FEM Calculation", IEEE International Conference on Power System Technology, Vol.4, pp.2660-2663, (13-17) Oct.2002.

[6]. E. Salinas, M. Rezinkina, J. Atalaya, "Some 2D-3D Aspects of Shielding of Longitudinal Sources of Extremely Low Frequency Magnetic Fields", Springer Science Environmentalist (2009) 29: 141-146

[7]. Aldo Canova, Alessandra Manzin, Michele Tartaglia, " Evaluation of Different Analytical and Semi-Analytical Methods for the Design of ELF Magnetic Field Shields", IEEE Transactions On Industry Applications, VOL. 38, NO. 3, pp.788-796, May/June 2002.

[8]. Republic of Iraq, Ministry of Electricity, "Iraq High Tension Projects 132/33/11/6.6 KV GIS Substations", Standard Specification Volumes (1,2 and 3), 2007.

[9]. Zhang Xiumin，Yuan Jinsha，Cui Xiang, "Edge-Nodal Coupled E-E- Ψ Method for Computing 3D Eddy Current Problems [J]", Proceedings of the CSEE, 23(5)： pp.70- 75, 2003.

[10]. Biro O , Preis K," On The Use of the Magnetic Vector Potential in the Finite Element Analysis of 3D Eddy Currents [J]". IEEE Trans. on Magnetics, 25(4), 1989.

[11]. Wassef K, Varadan VV, Varadan VK, "Magnetic Field Shielding Concepts for Power Transmission Lines", IEEE Transactions on Magnetic, Vol. 34, issue 3, pp.649-654, 1998.

[12]. Ooi Tian Hock, Foo Chew Houw B, "Automated Shielding Effectiveness Test System for Shielded Enclosures" Electromagnetic Compatibility (IEEE), pp.682-685, 1999.

Table (1): Parameters of the Busbar Finite Element Model

Model Parameters		Value
Cross-section		25.4*305mm^2
Length bar section		12.2m(40feet)
Minimum Clearance	Centerline-to- centerline phase spacing	0.914m
	To grounded parts	0.33m
	Between bare overhead& ground	3.05m
	Between bare overhead& roadways inside substation	6.71m
Material Properties of busbar (copper)	Relative permeability μ_r	1
	Conductivity σ	5.99*10^{7}S.m^{-1}
Air medium Relative permeability μ_r		1

Table(2): Parameters of shielding Finite Element Model

Model Parameters	**Value**
Thickness (y_s)	(3-10)mm
Width (x_s)	2m
Material Properties	
Relative permeability μ_r	
Aluminum	1
Copper	1
Ferromagnetic material (iron)	500
Conductivity σ	
Aluminum	$3.77*10^7 S.m^{-1}$
Copper	$5.99*10^7 S.m^{-1}$
Iron	$1.07*10^7 S.m^{-1}$

Table (3): Shielding effectiveness according to the distance *d* busbars to shielding plate at different points in XY plane.

X(m) Distance from center busbar system	**Y(m) Distance above floor**	**SE(dB)**		
		d=10cm	**d=15cm**	**d=20cm**
0.1	0.5	7.0984	4.2850	4.4717
1	0.75	10.4053	4.6120	3.8080
3.3	1	15.9246	5.6259	7.6626
2.5	1.25	9.5038	4.6872	5.5147
1.6	1.5	4.1163	2.9295	1.9253
-0.1	1.75	16.2943	20.6337	17.4529
-1.7	2	1.2411	1.4211	2.3876
-2.5	2.5	1.0176	1.3819	1.0066
-3.2	2.75	0.7317	3.1796	0.6986
0.3	3	12.3447	8.6110	9.8655

Table (4): Shielding effectiveness according to the thickness τ of the shielding plate at different points in XY plane.

X(m) Distance from center busbar system	Y(m) Distance above floor	SE(dB)		
		τ =3mm	τ =5mm	τ =10mm
0.5	0.5	10.4505	12.9258	11.7140
1.5	0.75	19.7117	6.5124	2.1306
3.3	1	22.0645	13.7177	7.2312
2.3	1.25	19.8650	10.2446	5.6658
1	1.5	2.5776	1.2506	0.2514
-0.2	1.75	0.5188	0.8136	1.1751
-1.6	2	0.8331	0.5591	2.4438
-3.3	2.5	2.2422	3.0719	2.1723
2	2.75	9.8481	11.8680	9.5243
2.5	3	13.7072	20.6961	9.4340

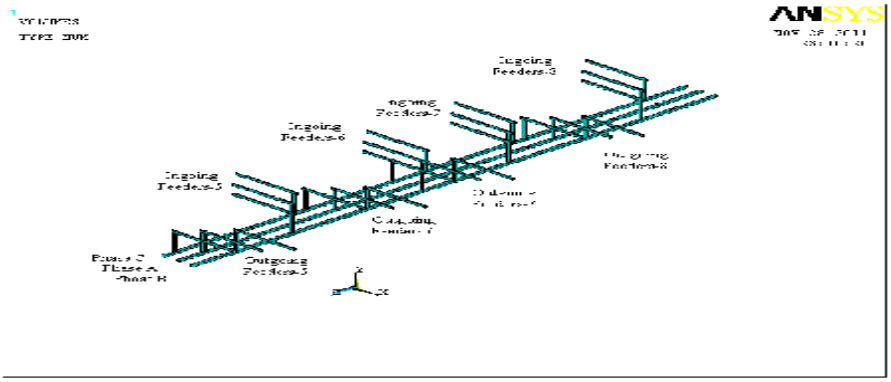

Figure (1): Busbar Area Model for Calculating Magnetic Field.

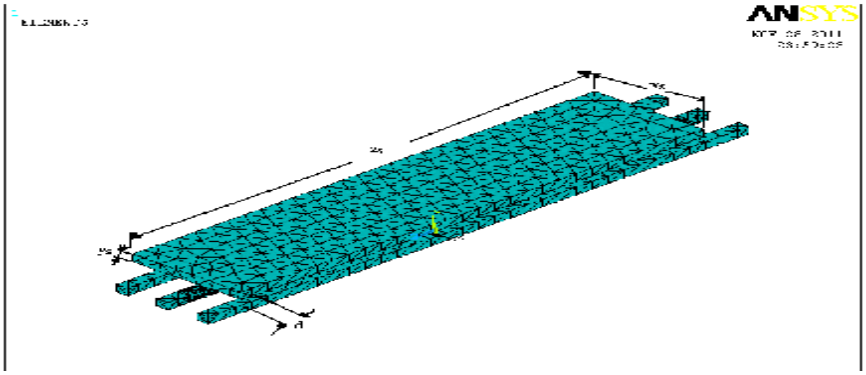

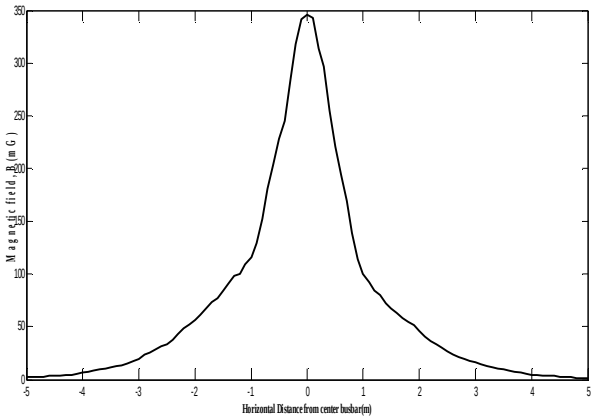

Figure (3): Magnetic Field at 1m above the Floor.

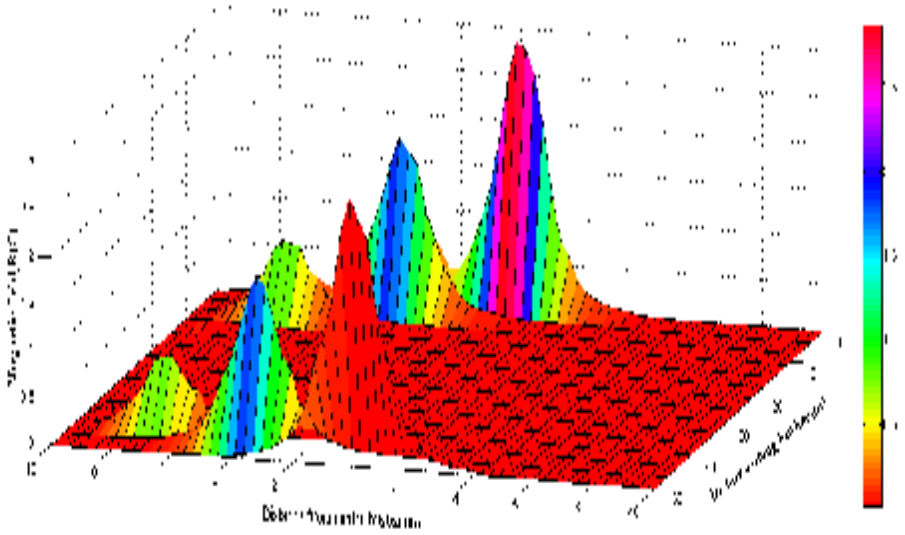

Figure (4): Magnetic Field Distribution at 1m Height on the Horizontal Plane XZ.

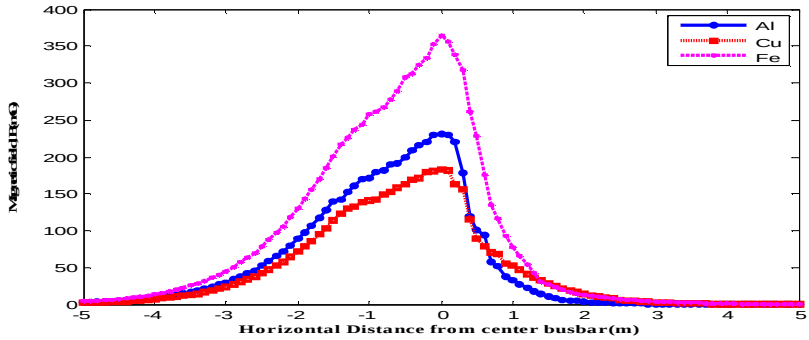

Figure (5): Magnetic Field at 1m above the Floor for Three Different Shielding Materials (Cu, Al &Fe).

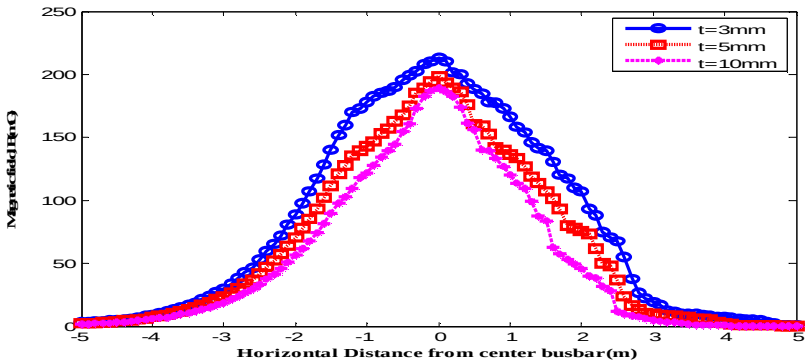

Figure (6): Variation of the Magnetic Field with Plate Thickness (τ).

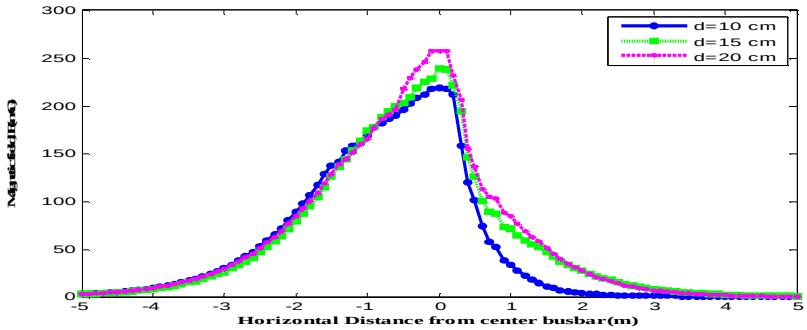

Figure (7): Variation of the Magnetic Field (at y=1) with Distance Aluminum Plate-Busbar *(d)*.

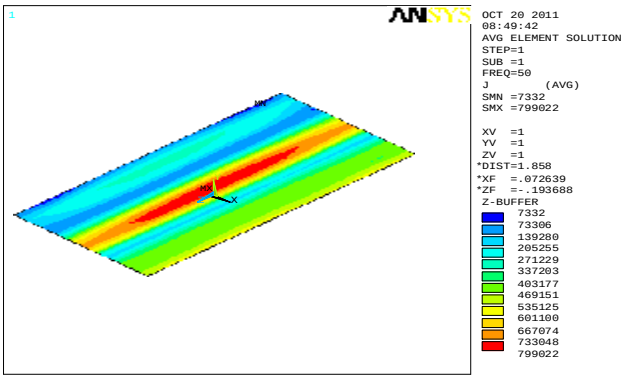

a) d=10cm

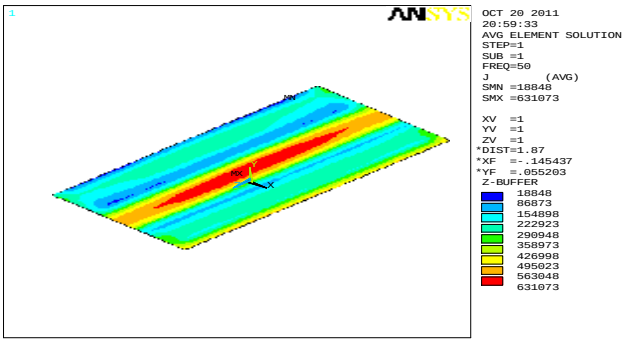

b) d=15cm

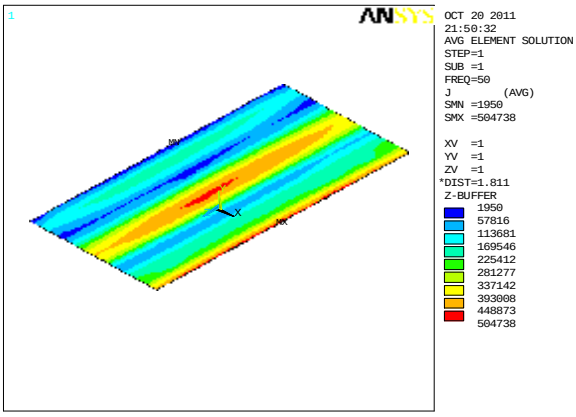

c) d=20cm

Figure (8): Distribution of the Eddy Current Density (A/m^2) on the Shielding Aluminum Plate for Different Distances *(d)*.

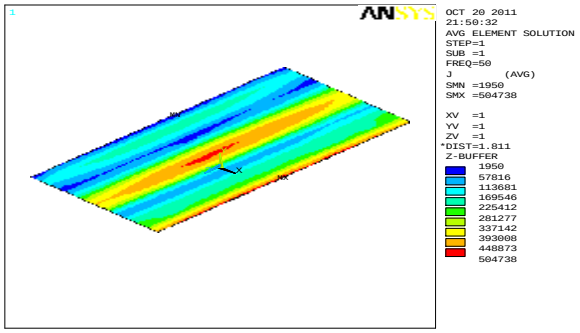

a) d=10cm

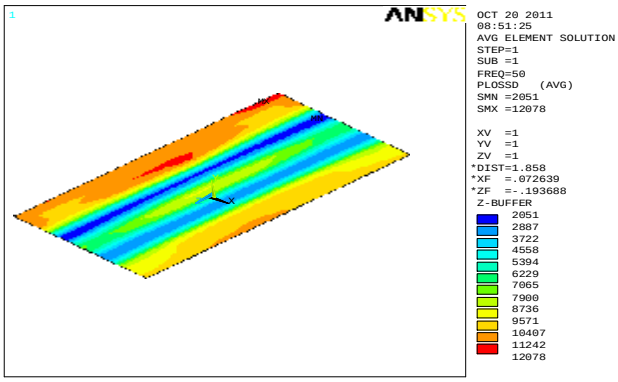

b) d=15cm

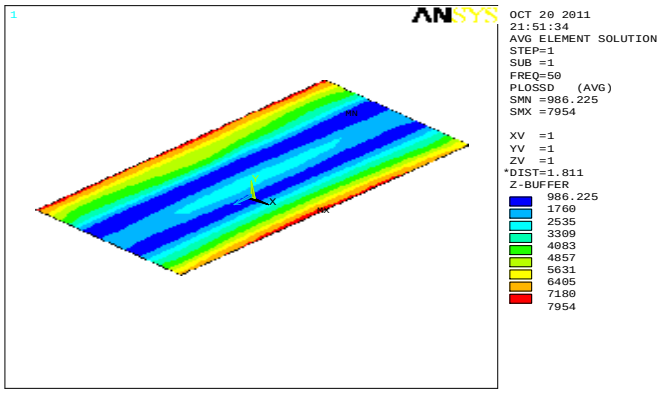

c) d=20cm

Figure (9): Distribution of the Power Loss (W/m) on the Shielding Aluminum Plate for Different Distances *(d)*.

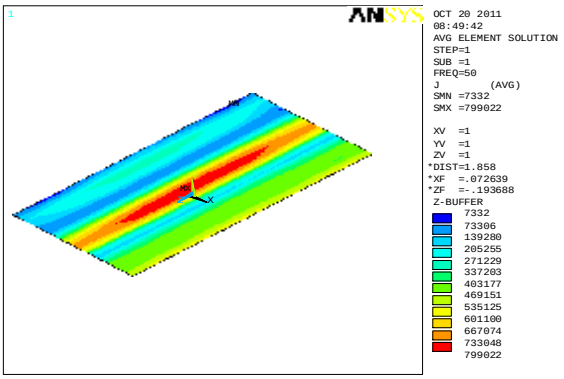

a)τ=3mm

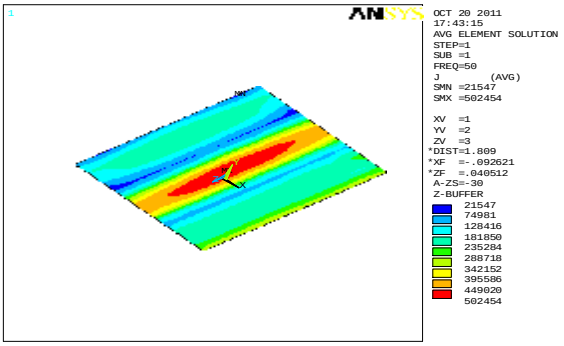

b)τ=5mm

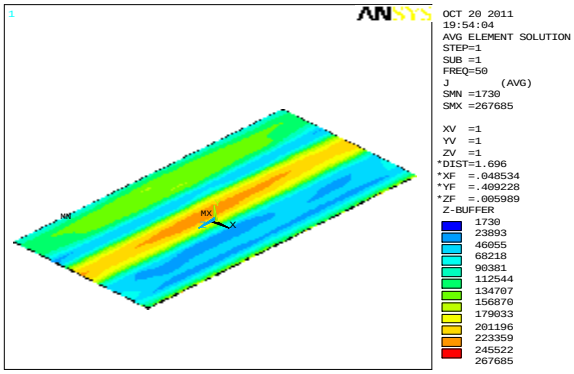

c)τ=10mm

Figure (10): Distribution of the Eddy Current Density (A/m^2) on the Shielding Aluminum Plate for Different Thickness *(τ)*.

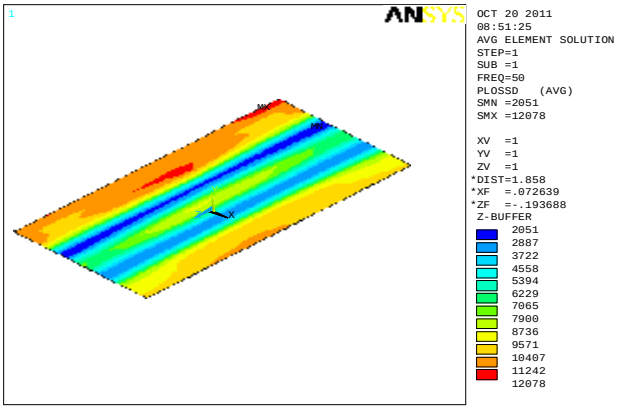

a)τ=3mm

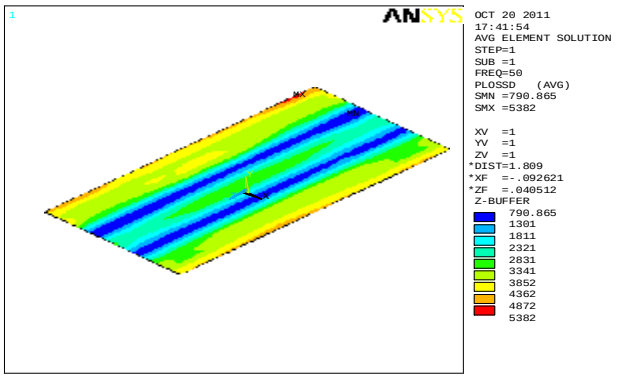

b)τ=5mm

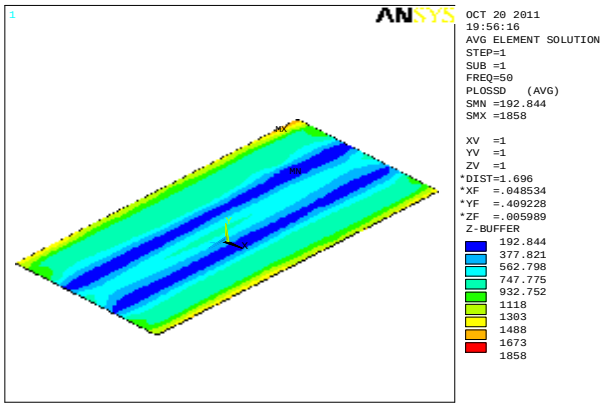

c)τ=10mm

Figure (11): Distribution of the Power Loss (W/m) on the Shielding Aluminum Plate for Different Thicknesses *(τ)*.